

High-resolution surface-sensitive C 1s core-level spectra of clean and hydrogen-terminated diamond (100) and (111) surfaces

R. Graupner, F. Maier, J. Ristein, and L. Ley

Institut für Technische Physik, Universität Erlangen, Erwin-Rommel-Strasse 1, 91058 Erlangen, Germany

Ch. Jung

BESSY GmbH, Lentzeallee 100, 14195 Berlin, Germany

(Received 24 October 1997; revised manuscript received 10 February 1998)

The carbon 1s core levels of diamond (100) and (111) surfaces were investigated using high-resolution photoelectron spectroscopy. The surfaces were prepared in a hydrogen plasma, which is known to result in atomically flat surfaces. From the signature of the C 1s core-level spectra, four different surface terminations can be distinguished. The as-prepared surfaces exhibit a surface component shifted by +0.5 to +0.8 eV toward higher binding energy, which we assign to multiple termination of carbon atoms by hydrogen. Annealing these surfaces first results in the development of the surfaces terminated monoatomically by hydrogen. A small chemical shift of -0.15 eV was deduced for the hydrogen-terminated surface atoms of the (111):H surface with respect to the bulk carbon atoms. Further annealing leads to spectra characteristic for hydrogen-free, reconstructed diamond surfaces. This process is shown to be thermally activated with an activation energy of 3.4 ± 0.4 eV. The corresponding chemical shifts between surface and bulk components vary between -0.78 and -1.15 eV depending on surface orientation and surface treatment. Finally, annealing at $T \approx 1250$ °C leads to a partially graphitized surface for diamond (111) while on the diamond (100) surface a 4×1 reconstruction is observed. The sign and magnitudes of the chemical shifts are discussed. [S0163-1829(98)11119-0]

I. INTRODUCTION

Virtually all materials exhibit core-level binding energies of their surface atoms that differ from those of the corresponding bulk atoms. These surface chemical shifts reflect the charge redistribution and—for ionic compounds—the change in Madelung potential that accompanies the reduction in the number of nearest neighbors at the surface and any atomic reconstruction that the material undergoes in order to minimize its surface energy. As such, the measurement and analysis of surface chemical shifts provides valuable information about the structure and bonding arrangements at crystal surfaces. On semiconductor surfaces different components in core-level spectra are usually attributed to inequivalent atom sites.¹ A case in point is, for example, the work of Landmark *et al.*² performed on the Si(100) (2×1)-reconstructed surface. Utilizing high-resolution photoelectron spectroscopy (PES) with synchrotron radiation, they were able to resolve four chemically shifted surface components on the Si 2p core line which they attributed to emission from inequivalent surface and subsurface atoms on the basis of charge transfer arguments, and the intensities of the surface components relative to the unshifted bulk line. Similar measurements were performed on the Si(111) 7×7 surface, where four³ or five⁴ surface components could be assigned to the inequivalent surface atoms, again based mainly on charge-transfer arguments. On hydrogen-terminated Si(111) surfaces, the total number of surface components is not yet clear.^{5,6} With a similar intention, here we present a study of the C 1s core-level spectra of the clean and hydrogen-terminated (111) and (100) surfaces of single-crystalline diamond using high-resolution PES.

Diamond surfaces are usually prepared by mechanical polishing or exposure to atomic hydrogen at elevated temperatures (800–900 °C). Both preparation techniques lead to (at least partially) hydrogen-terminated surfaces. Clean diamond surfaces are obtained by annealing these surfaces above the hydrogen desorption temperature at 900–1200 °C in UHV.

The (100) surface prepared that way shows a 2×1 reconstruction. The structural model of this surface consists of dimers, similar to that of the Si(100) surface. In contrast to the Si surface, however, symmetric dimers are predicted for the diamond (100) surface.^{7–12} The bonding between the dimer atoms can be viewed as a double bond (π plus σ bond).^{7,13} By adsorption of one hydrogen atom per surface C atom (coverage $\Theta = 1$) the π bond is broken. The dimers are still present, and the bond distance corresponding to a single bond (σ bond) is enlarged. The resulting surface structure is the monohydrogenated, 2×1 -reconstructed (100) surface, C(100) 2×1 :H. Surfaces prepared by a microwave hydrogen plasma¹⁴ or grown homoepitaxially¹⁵ are believed to exhibit that kind of surface termination. Support for this comes from high-resolution electron-energy-loss spectroscopy (HREELS),^{15,14} scanning tunneling microscopy (STM),^{16,17} and low-energy electron diffraction (LEED).^{18,19} In principle, one can also imagine a bulklike termination of the diamond (100) surface with two hydrogen atoms per surface atom ($\Theta = 2$). However, the distance between two H atoms on adjacent surface atoms would be very small. Therefore, it is not yet clear whether this surface structure exists²⁰ or not exists,^{10,21,22} as the observed 1×1 LEED pattern on mechanically polished surfaces^{23–25} taken as a confirmation for the C(100) 1×1 :2H surface might just reflect the symmetry

TABLE I. Results of the C $1s$ core-level analysis for the (100) surface of diamond. ΔE refers to the binding-energy shift of the surface component relative to the bulk component, w_G to the width (FWHM) of the Gauß component in the line fits, and % to the relative contribution of each component to the total emission intensity. The asterisk marks values that have not been varied during the fit.

(100) surface	$\hbar\omega$ (eV)	Component	ΔE (eV)	w_G (eV)	%
as prep. $T_{\text{prep}} \approx 800$ °C	325	Surface S_A	$+0.50 \pm 0.03$	1.08	34
		Bulk B	—	0.41	66
	305	Surface S_A	$+0.50^*$	0.72	19
		Bulk B	—	0.40	81
as prep. $T_{\text{prep}} \approx 900$ °C	325	Surface S'_A	$+0.81 \pm 0.01$	0.81	55
		Bulk B	—	0.45	45
ann. at 700 °C	325	Bulk B	—	0.51	100
ann. at 1050 °C	325	Bulk B	—	0.51	62
		Surface S_C	-0.90 ± 0.01	0.55	38
	305	Bulk B	—	0.49	82
		Surface S_C	-0.90^*	0.54	18

of the bulk material beneath a disordered surface.¹⁴ Besides the monohydrogenated and the dihydrogenated (100) surfaces, ordered hydrogen terminations with $1 < \Theta < 2$ were considered as well.^{9,10,13,20,21,26} However, no experimental evidence for these structures is available as yet.

The diamond structure viewed perpendicular to the [111] direction consists of bilayers separated by the bond distance. Cutting a crystal between the bilayers leads to the single dangling-bond surface, the cleavage plane of the diamond structure. The 2×1 reconstruction observed on clean diamond (111) surfaces is usually explained in terms of the π -bonded chain model of Pandey.²⁷ A termination of every surface atom by one hydrogen atom leads to a bulklike surface structure. Again, these surfaces can be prepared by plasma techniques [homoepitaxial growth, H plasma at 800–900 °C (Refs. 19 and 28)].

The (111) surface which is formed by cutting the bilayers yields three dangling bonds per surface atom (triple dangling bond surface). Two reconstructions are predicted for this surface which are similar in total energy. One is the (2×1) -reconstructed Seiwatz single-chain model,^{29,30} and the other consists of trimers which would form a $(\sqrt{3} \times \sqrt{3})R30^\circ$ structure.^{21,29,30} A complete hydrogenation of the triple dangling-bond surface corresponds to a single dangling-bond surface completely terminated by methyl radicals.²⁹

Earlier core-level studies by photoelectron spectroscopy were performed on the (111) (Refs. 31–34) and (100) surfaces of diamond.^{35–38} The general consensus appears to be as follows: The as polished or *ex situ* cleaved surface has, in addition to the dominant bulk C $1s$ line, some tailing toward higher binding energy,³² that is in some cases interpreted as one or more separate components shifted towards higher binding energy.^{31,33} In an earlier paper we attributed this surface core-level shift to adsorbed CH_2 or CH_3 species.³³ The asymmetric tailing is removed at temperatures below the temperature necessary to desorb hydrogen.³² Upon annealing at or above the hydrogen desorption temperature, a line appears at lower binding energy in all cases including the (100)

surface. Its intensity relative to the bulk component scales with the mean free path of the photoelectrons, as expected for emission from the diamond surface. This surface core-level peak is thus considered characteristic of the hydrogen-free reconstructed (111) and (100) surfaces of diamond. However, different magnitudes for the chemical shifts have been reported in the literature that range from 0.8 (Refs. 32 and 34) to 0.95 eV (Ref. 31) on the (111) surface and from 0.9 (Refs. 35 and 36) to 1.2 eV (Ref. 37) on the (100) surface. An exact value as well as a model accounting for the sign and magnitude of the surface core level shift is lacking up to now.

The paper is organized as follows: After a description of the sample preparation and the experimental conditions in Sec. II, we present the C $1s$ core-level spectra for differently treated (111) and (100) surfaces in Sec. III. In Sec. IV we attempt an identification of the observed surface core-level shifts, and we conclude with a summary in Sec. V.

II. EXPERIMENTAL ASPECTS

A. Sample preparation

The samples used were commercially available type-IIb diamond single crystals which had boron concentrations of about $1 \times 10^{16} \text{ cm}^{-3}$, and were thus sufficiently conductive to avoid any charging problems during PES measurements. The as-received crystals had mechanically polished (100) and cleaved (111) surfaces of about $3 \times 5 \text{ mm}^2$ area. In one case we also used a mechanically polished (111) surface. At this stage the samples showed very few oxygen containing surface contaminants as judged by XPS (x-ray-induced photoelectron spectroscopy), that could be completely removed by annealing at ≈ 600 °C, and they showed a 1×1 LEED pattern. Annealing above 950 °C converted both types of surfaces to a 2×1 reconstruction, as expected. However, angle-resolved photoemission measurements of the valence

TABLE II. Same as Table I for the (111) surface. The asterisk marks values that have not been varied during the fit.

(111)-Surface	$\hbar\omega$ (eV)	Component	ΔE (eV)	w_G (eV)	%
as prep. $T_{\text{prep}} \approx 800$ °C	325	Surface S_A	$+0.70 \pm 0.02$	0.75	41
		Bulk B	—	0.53	59
as prep. $T_{\text{prep}} \approx 900$ °C	325	Surface S'_A	$+0.75 \pm 0.01$	0.79	65
		Bulk B	—	0.46	35
light ind. desorption	325	Surface S'_A	$+0.75^*$	0.73	26
		Bulk B	—	0.68	74
ann. at 850 °C	325	Bulk B	—	0.55	93
		Surface S_C	-1.02^*	0.77*	7
ann. at 1050 °C	325	Bulk B	—	0.62	45
		Surface S_C	-1.02 ± 0.01	0.77	55
	305	Bulk B	—	0.62	59
		Surface S_C	-1.02^*	0.94	41
ann. at 1250 °C	325	Bulk B	—	0.82	30
		Surface S_D	-1.13 ± 0.02	0.47	70
	305	Bulk B	—	0.82	41
		Surface S_D	-1.13^*	0.55	59

bands showed virtually no features dispersing with emission angle, and we therefore considered these surfaces insufficiently ordered. The surface quality was markedly improved after “polishing” the samples in a hydrogen plasma as suggested by Thoms *et al.*¹⁸ and Küttel *et al.*¹⁹ To this end, the surfaces were exposed at a temperature of about 800–900 °C for 10–15 min to a hydrogen plasma maintained by a microwave discharge in 50 mbar of H₂. This treatment which can be repeated a few times yields clean (as judged by XPS) and, according to Ref. 19, atomically flat surfaces on which the 2 × 1 dimerization has been observed for the (100) surface by scanning tunnelling microscopy.¹⁷ Before and after dehydrogenation at ≈ 950 °C, the (111) and (100) surfaces exhibit sharp and strongly dispersing bulk and surface states, as has been demonstrated elsewhere.³⁹ It is these plasma-polished surfaces that we used for our present investigation. The diamond crystals were mounted on a thin Ta foil, and could be heated by electron bombardment of the Ta foil from the back. In the high-temperature regime the actual diamond temperature is expected to be considerably lower. In a control experiment where we placed a Ta sample in place of the diamond specimen to mimic the heat contact between sample and support, we measured pyrometrically a temperature difference of about 150 °C between the dummy Ta “sample” and the Ta sample support. The temperatures quoted throughout this paper are therefore the pyrometric temperatures of the Ta sample support reduced by 150 °C. Even with this correction there is a considerable error margin in the diamond temperatures of an estimated ± 50 °C.

B. Photoemission setup and data treatment

The PE spectra were recorded with a hemispherical electron energy analyzer at the Berlin synchrotron radiation source BESSY. A plane-grating monochromator (Petersen

monochromator) set to a resolution of 120 meV at $\hbar\omega = 300$ eV (slit width 100 μm) was used to excite the C 1s core electrons. We chose two photon energies, 325 and 305 eV, which yield kinetic energies of the C 1s photoelectrons of ≈ 35 and 15 eV, respectively. At a kinetic energy of 35 eV we are near the minimum in the electron escape depth (3–4 Å), and the spectra are thus termed “surface sensitive.” At 15 eV the electron mean free path is expected to be around 10 Å, and the spectra are termed “volume sensitive.” The overall resolution (monochromator and electron analyzer) of the core-level spectra is estimated to be ≈ 130 meV. The background of inelastically scattered electrons which is steeply rising at low kinetic energies was corrected for by recording the same electron energy spectrum, albeit with a photon energy lower than the emission threshold of the C 1s core level ($\hbar\omega = 285$ eV), and subtracting the two spectra from each other. The remaining background could—whenever necessary—be removed by applying Shirley’s method.⁴⁰ The spectra so corrected were fitted with convolutions of Gaussian and Lorentzian line shapes (Voigt functions). The smallest value we obtained for the Lorentz width Γ_L was 0.15 eV (full width at half maximum, FWHM) which was subsequently kept fixed in all fits. The width of the Lorentz line reflects the lifetime of the C 1s core hole, and we had no indication that this lifetime was affected in a reproducible and consistent way by the electronic structure of the surface. The value of 0.15 eV for Γ_L is slightly smaller than the 0.18 eV reported by Morar *et al.*,³² but still higher than the theoretical estimate of ≈ 0.1 eV.⁴¹ Energies in the core-level spectra will be quoted as binding energies relative to the C 1s bulk component.

III. RESULTS

Because the core-level spectra for the (111) and (100) surfaces differ only in detail, we shall discuss them in paral-

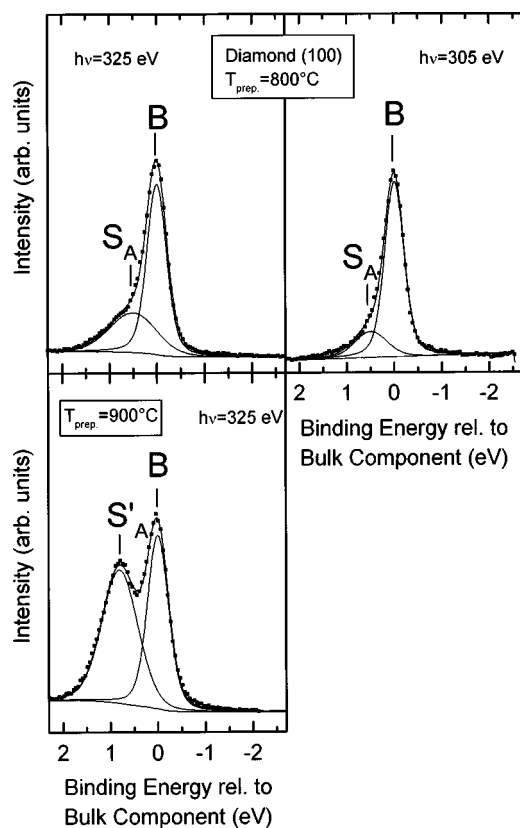


FIG. 1. C 1s core-level spectra of a diamond (100) surface prepared in a microwave hydrogen plasma. Top: prepared at $T \approx 800$ °C (left: $\hbar\omega = 325$ eV, surface sensitive; right: $\hbar\omega = 305$ eV, bulk sensitive). Bottom: prepared at $T \approx 900$ °C ($\hbar\omega = 325$ eV, surface sensitive).

l. All relevant data derived from the line-shape analysis are gathered in Tables I and II, and we will refer to these tables frequently in what follows. In order to facilitate the discussion, we present our results by defining four different surface phases. Phase A is that immediately after the plasma treatment. Phase B is obtained after annealing at a temperature between 450 and 850 °C, and is characterized by a single C 1s component. Phase C is obtained after driving off the hydrogen at temperatures above 950 °C, and, in phase D, finally, graphitization of the diamond (111) surface sets in after annealing at ≈ 1250 °C. All annealing steps were performed *in situ*, and the data presented below were taken at room temperature. The surfaces were routinely checked for contamination by monitoring the core-level intensities of the prevailing adsorbates. It was found that the diamond surfaces were in general exceptionally clean with no detectable contamination. Exceptions from the rule will be pointed out.

Phase A: the surface after plasma preparation

The upper two spectra in Fig. 1 show the C 1s spectral region of a (100) surface after plasma preparation at a temperature of 800 °C. In addition to the bulk C 1s line (labeled B) a component shifted by $\Delta E = +0.5$ eV toward higher binding energies is clearly distinguishable (S_A in Fig. 1). The fact that the contribution of this component relative to the total C 1s emission increases from 19% to 34% as the photon energy changes from 305 (bulk sensitive) to 325 eV (sur-

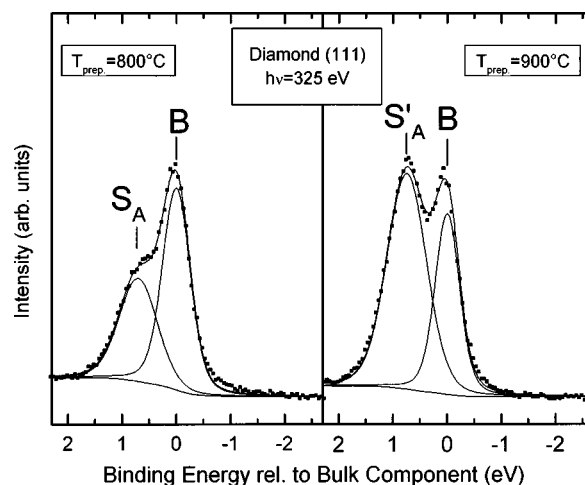


FIG. 2. C 1s core-level spectra of a diamond (111) surface, $\hbar\omega = 325$ eV. Left: prepared at 800 °C, right: prepared at 900 °C.

face sensitive) confirms that this extra emission stems from the diamond surface. The intensity and chemical shift of this surface component depends sensitively on the preparation conditions. After a different plasma treatment (nominally

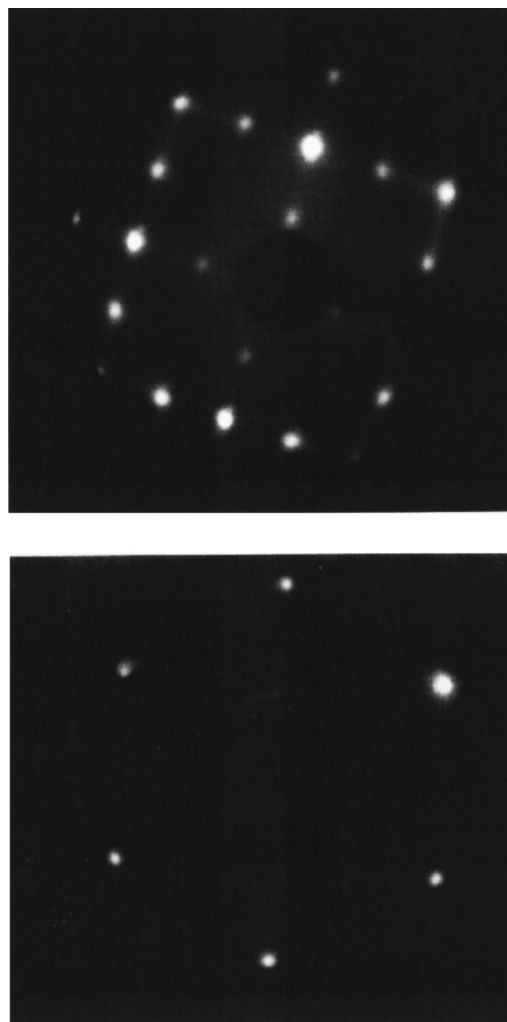


FIG. 3. Top: LEED pattern of the as-prepared diamond (100) surface, $E = 94.3$ eV. Bottom: LEED pattern of the as-prepared diamond (111) surface, $E = 75.7$ eV.

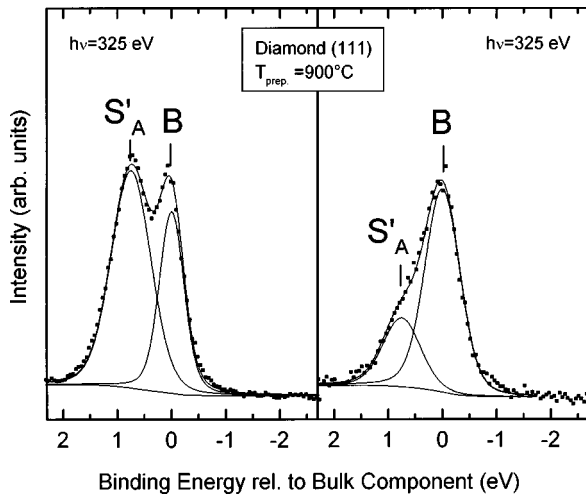


FIG. 4. C 1s core-level spectra ($\hbar\omega = 325$ eV) of a diamond (111) surface. Left: as prepared, right: after several hours of illumination with soft x rays ($\hbar\omega > 285$ eV).

with a somewhat higher substrate temperature of ≈ 900 °C), a component S'_A (Fig. 1, lower spectrum) arises that is shifted by +0.81 eV and contributes 55% to the total C 1s intensity in the “surface-sensitive” 325-eV spectrum (also compare Table I). The situation is analogous for the (111) surface. After plasma polishing at 800 °C a surface component S_A shifted by +0.70 eV with a relative contribution of 41% is measured at $\hbar\omega = 325$ eV (see Fig. 2) that is replaced after a 900 °C plasma preparation step by S'_A ($\Delta E = +0.75$ eV) that now contributes a remarkable 65% to the spectrum. For the (100) surface, a sharp LEED pattern of a (2×1) -reconstructed surface with low background intensity is observed (Fig. 3, upper picture). The LEED pattern of the (111) surface corresponds to a well ordered, 1×1 surface unit mesh (Fig. 3, lower picture). For both surfaces the different preparation temperatures do not lead to a visible change in the LEED pattern.

The species responsible for the surface core-level shift is apparently sensitive to light induced desorption. In Fig. 4 we

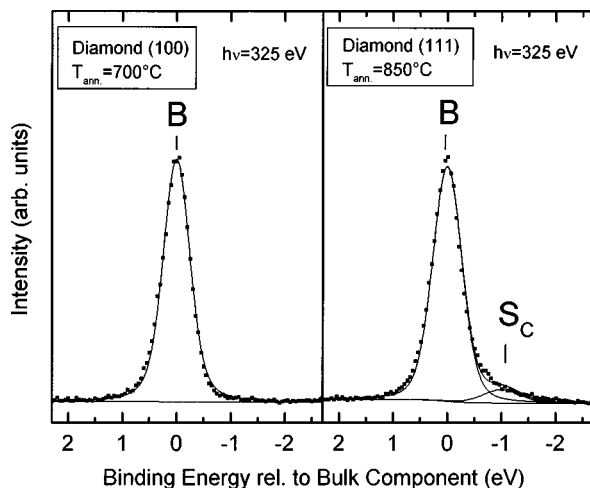


FIG. 5. Left: C 1s core-level spectrum of a diamond (100) surface annealed at 700 °C, right: C 1s core-level spectrum of a diamond (111) surface annealed at 850 °C, $\hbar\omega = 325$ eV.

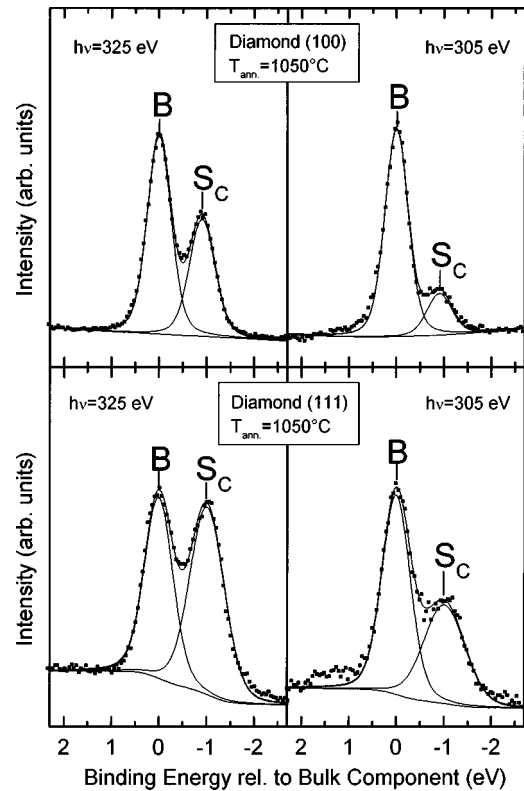


FIG. 6. C 1s core-level spectra of diamond surfaces annealed at 1050 °C. Top: (100) surface (left: $\hbar\omega = 325$ eV, surface sensitive; right: $\hbar\omega = 305$ eV, bulk sensitive). Bottom: (111) surface (left: $\hbar\omega = 325$ eV, surface sensitive; right: $\hbar\omega = 305$ eV, bulk sensitive).

compare spectra taken from the same (111) surface at the beginning of a series of measurements (left-hand side) and after several hours of exposure to radiation above 285 eV (right-hand side). The intensity of the surface component has dropped to about half its initial value without a discernible change in chemical shift. Remarkable, however, is that the Gaussian width of the bulk component is markedly increased from about 0.5 eV in all previous spectra to 0.68 eV after light-induced desorption (see Table II). This points either toward an inhomogeneous broadening reflecting an extrinsic subsurface disorder induced by the desorption process, or to the fact that the larger width is due to intrinsic surface components with chemical shifts too small to be resolved. We will return to this point below. The electron diffraction pattern remains unchanged: 1×1 .

Phase B: after annealing at 700 °C

The spectrum on the left-hand side of Fig. 5 shows the C 1s spectrum of the diamond (100) surface after it had been annealed at 700 °C for 5 min. It consists of a single line without a resolved surface component, despite the fact that the spectrum was taken in the surface-sensitive mode. The Gaussian width (FWHM) amounts to 0.51 eV, which is comparable to the width measured for the diamond (111) surface after annealing at 850 °C [0.55 eV, Fig. 5, right-hand side]. After this higher annealing temperature a small component S_C on the low-binding-energy side has evolved that will be discussed in Sec. IV. Here we obviously missed the optimum

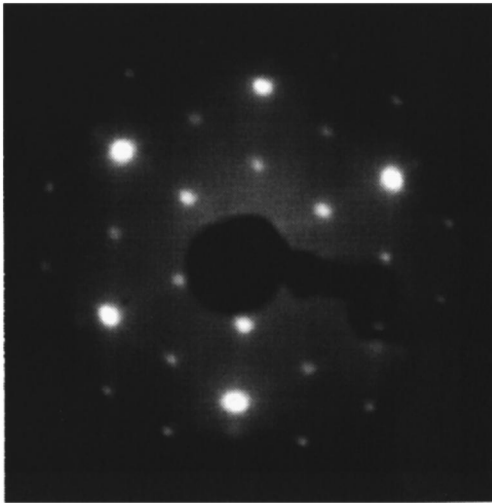


FIG. 7. LEED pattern of a diamond (111) surface annealed at 1050 °C, $E=106$ eV.

annealing temperature and went beyond the point where component S_A has vanished completely without there being any new component to appear. It is, nevertheless, safe to assume that also on the (111) surface a phase B exists that is characterized by the absence of any resolved component which can be attributed to the emission from surface atoms. It is also remarkable that the LEED pattern remains unchanged in going from phase A to phase B: it remains 2×1 on (100) and 1×1 on (111).

Phase C: after annealing at 1050 °C

Annealing both diamond surfaces at 1050 °C for 10 min yields the spectra depicted in Fig. 6. Now in both cases a surface core-level shift towards lower binding energy appears in addition to the bulk C 1s component (S_C in Fig. 6). Its origin from the surface is again demonstrated by the doubling in relative intensity of S_C in going from 305-eV photon energy to 325 eV. Despite these similarities there are differences in detail for the two surfaces. On the (100) surface, the chemical shift of S_C is -0.90 eV, whereas it is -1.02 eV on (111). Also the intensities differ. For $\hbar\omega=325$ eV, $I_{S_C}/(I_B+I_{S_C})$ is 0.38 on (100), whereas the same ratio is 0.56 on (111). However, an attempt to quantify the intensities on the basis of an inelastic scattering length gave no consistent results because the probe depths in this experiment were extremely small ($\approx 3-10$ Å). With this annealing step the LEED pattern of the (111) surface changes from 1×1 to 2×1 , indicating that a reconstruction of the surface has taken place as observed previously (see Fig. 7). The surface unit mesh of the (100) surface remains 2×1 (not shown). The spectra of the (111)-oriented sample discussed so far were obtained on a cleaved surface after it had been subjected to the hydrogen plasma treatment at elevated temperatures. A remarkable difference in the C 1s spectrum of phase C is observed if a polished (111) surface is subjected to the same treatment. The spectra of a cleaved and a polished (111) surface are superimposed in Fig. 8, and they demonstrate that the surface core-level shift is substantially larger on the cleaved surface, compared to the polished surface. To obtain a consistent fit of both spectra, one has to

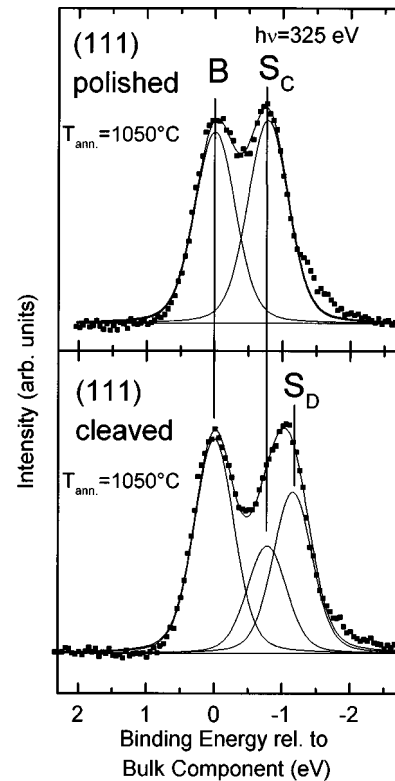


FIG. 8. C 1s core-level spectra of two different (111) surfaces, plasma hydrogenated and annealed at 1050 °C, $\hbar\omega=325$ eV. Top: polished sample; bottom: cleaved sample.

assume that the surface component indeed consists of at least two components (S_C and S_D , Table III). On the polished (111) surface only one of them is visible, shifted by $\Delta E = -0.78$ eV from the bulk component. For the cleaved surface a second surface component S_D with a larger chemical shift ($\Delta E = -1.15$ eV) has to be introduced, which is even the dominant one in that case. It should be mentioned that this component is not responsible for the slight shoulder on the low-binding-energy side of the C 1s signal from the polished sample which is situated at even higher binding energy but was not investigated further (Fig. 8, upper panel).

In Fig. 9 the transition from phase B to phase C is investigated in detail for the polished (111) surface. To this end the sample was annealed at temperatures increasing from 850 °C in steps of 50 °C (25 °C between 1000 and 1050 °C) up to 1100 °C, and kept at each temperature for 3 min. Following each step the sample was allowed to cool for 7 min, and the C 1s core-level spectrum was measured. Each spectrum was at first fitted to the two Voigt functions already shown in Fig. 8 (upper spectrum). The position of component B as well as the development of the relative intensity of component S_C as a function of annealing temperature are summarized in Fig. 10. It is evident from these figures that the phase transition that is signified by the evolution of the surface component S_C is thermally activated, and occurs between 850 and 1050 °C. At the same time the phase transition is accompanied by an increase in downward band bending of 0.5 eV, as witnessed by the corresponding increase in the binding energy of peak B in Fig. 10. A closer look at the spectra of Fig. 9 reveals an increase in the chemical shift of S_C from -0.65 eV at low intensity to -0.78 eV at the satu-

TABLE III. Same as Table I for the cleaved and polished (111) surface after 1050 °C anneal. The asterisk marks values that have not been varied during the fit.

(111)-surface	$\hbar\omega$ (eV)	Component	ΔE (eV)	w_G (eV)	%
polished	325	Bulk	—	0.62	49
		Surface	-0.78*	0.62	51
cleaved	325	Bulk	—	0.58	45
		Surface	-0.78*	0.60*	22
		Surface	-1.15	0.59	33

ration intensity of S_C . The reason for the change in energy separation between S_C and B is likely due to the fact that B consists of two unresolved components (B_{bulk} and B_{surf}) which we assign to the atoms of the first atomic layer, i.e. to the true surface atoms (B_{surf}), and to all subsurface atoms (B_{bulk}). The surface atoms are those which are involved in the phase transition from phase B to phase C, thus B_{surf} completely vanishes from B in the course of that transition and transforms into S_C . When B_{surf} and B_{bulk} differ slightly in peak position, an apparent shift of the peak maximum of B is expected which then leads to a corresponding change in the chemical shift between S_C and B . A consistent fit of all spectra shown in Fig. 9 is possible if one assumes that the separation between surface (B_{surf}) and bulk component (B_{bulk}) in peak B is 0.15 eV with the true bulk component (B_{bulk}) on the high-binding-energy side (see Fig. 11). The evolution of a nonresolved surface component B_{surf} might also be responsible for the broadening of B caused by the light induced decrease of S'_A in Fig. 4. Note the substantial constraints that have been imposed on the fit sequence of Fig. 11 and which make the extracted binding energy shift between B_{surf} and B_{bulk} very reliable even when not resolved directly: (i) all line positions and linewidths were held constant except for the overall shift due to band bending (see above); (ii) component B_{bulk} had to be constant in intensity; (iii) the combined intensity of B_{surf} and S_C had to be constant as well.

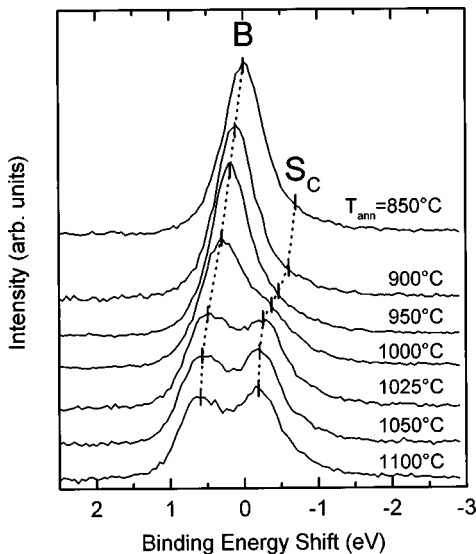


FIG. 9. Development of the C 1s core-level spectra of the polished (111) diamond surface upon annealing, $\hbar\omega = 325$ eV. The bulk component of the 850 °C spectrum was taken as zero for the relative binding-energy scale of the abscissa.

It should be mentioned that after heating at $T = 1000$ °C the LEED pattern, which has been routinely checked after each annealing step, showed a weak 2×1 reconstruction for the first time. The intensity of the half order spots increased up to $T = 1050$ °C. Further annealing only led to an increase of diffuse background (see below).

Phase D: annealing above 1050 °C and graphitization

For annealing temperatures of ≈ 1250 °C further changes in the C 1s spectra of the (111) and (100) surfaces are observed. On (111), the intensity ratio of surface component (labeled S_D in Fig. 12) to bulk component almost doubles (compare the lower set of spectra in Fig. 6 with Fig. 12) and the surface chemical shift increases further to -1.13 eV (see Table I). The comparison of the two spectra taken at 325 and

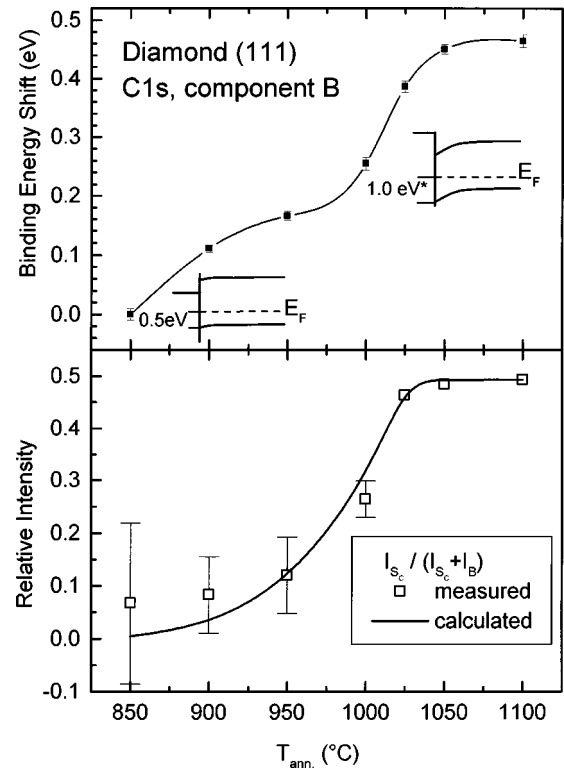


FIG. 10. Top: Binding-energy shift of the C 1s bulk component due to the change in band bending as a function of temperature. *The asterisk indicates the value of $E_F - E_{\text{VBM}} = 1.0$ eV for the hydrogen-free surface taken from Ref. 39. Bottom: Relative intensity of the surface component S_C in the C 1s core-level spectra as a function of temperature. The line was calculated assuming first-order desorption kinetics as explained in the text.

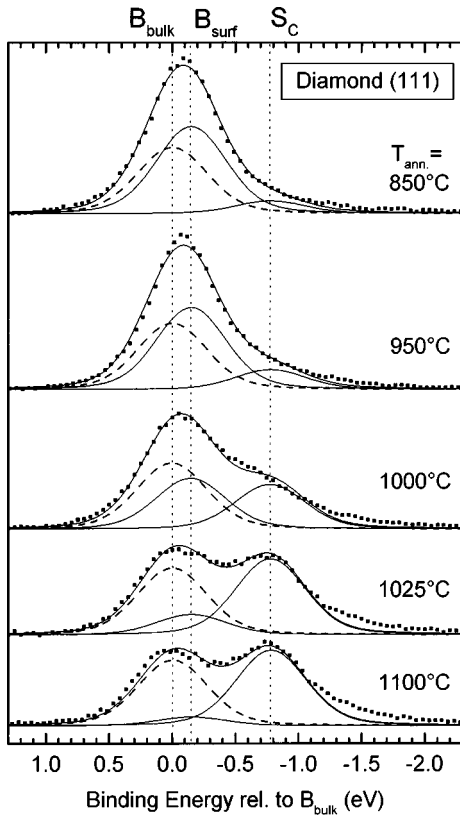


FIG. 11. Fit of C $1s$ core-level spectra shown in Fig. 9 by using three components. B_{bulk} : bulk component; B_{surf} : surface component of the monohydrogenated (111) surface; S_C : surface component of the hydrogen-free (111) surface.

305 eV, respectively, confirms nevertheless that the species responsible for S_D reside at the surface. This implies that a rearrangement of the surface has taken place which involves more than just the top layer. Notice also that the width of the bulk component has increased appreciably from 0.5–0.6 eV (FWHM) in the previous spectra to 0.82 eV after annealing at 1250 °C while the surface component has substantially narrowed in the last step: from 0.94 eV in Fig. 6 after the 1050 °C anneal to 0.47 eV now. The LEED pattern remains

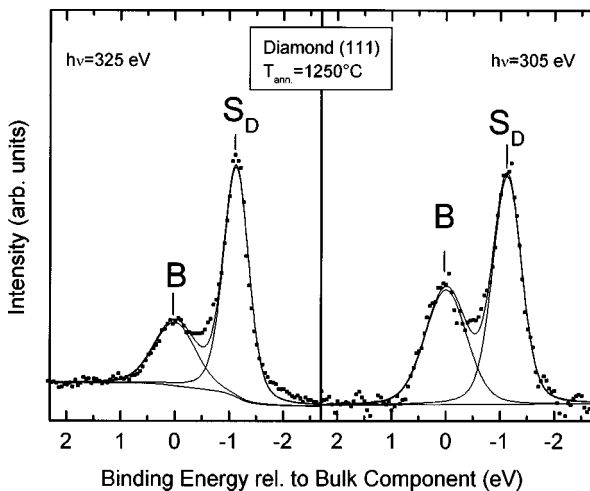


FIG. 12. C $1s$ core-level spectra of the diamond (111) surface annealed at 1250 °C. Left: $\hbar\omega = 325$ eV; right: $\hbar\omega = 305$ eV.

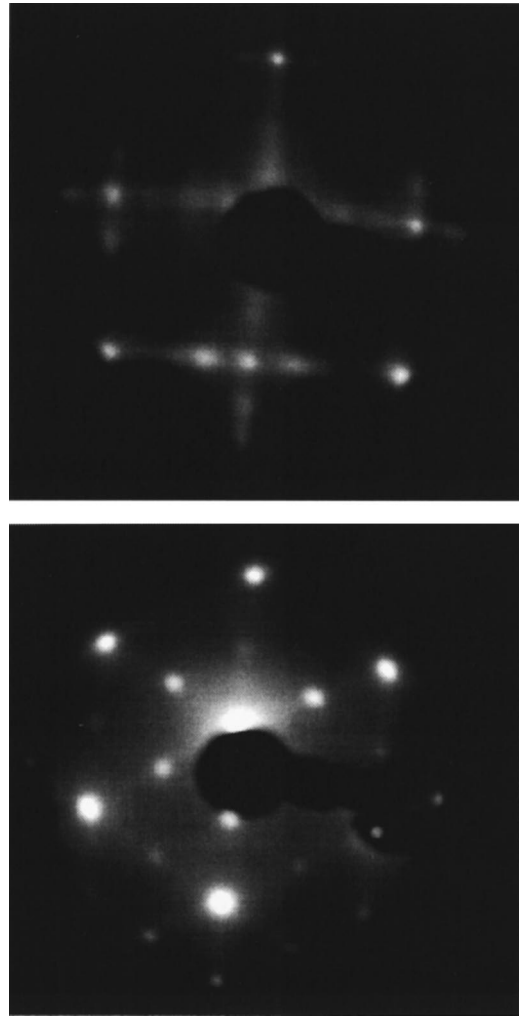


FIG. 13. Top: LEED pattern of a diamond (100) surface annealed at 1250 °C, $E = 101$ eV. Bottom: LEED pattern of the diamond (111) surface annealed at 1250 °C, $E = 106$ eV. Notice the increase in background intensity compared to Fig. 7.

2×1 , but the background increases considerably, and streaks develop between first-order spots as demonstrated in the lower picture of Fig. 13. Annealing the (100) surface at 1250 °C also leads to an increase in the surface component S_C but much less pronounced compared to (111). However, the LEED pattern has turned into that of a 4×1 reconstruction with marked streaking (Fig. 13, upper picture). Such a reconstruction has to our knowledge not been published for diamond (100) so far.

IV. DISCUSSION

A. Identification of phases A–D

The most studied diamond surfaces so far are the clean, (2×1)-reconstructed (111) and (100) surfaces. The core-level spectra of both surfaces exhibit a surface component shifted by ≈ 0.9 eV toward lower binding energies. If we compare the literature data with our measurements, we can identify phase C with the clean diamond surfaces. Strong support for this assignment stems from the fact that on surfaces which were prepared in the very same way the intrinsic

surface state dispersions were observed in angle-resolved photoemission, which was demonstrated elsewhere.³⁹

The surface structures which lead to the characteristic spectra of phases A and B are not nearly as clear. In all cases surface atoms other than C and H were below the detection limit of XPS. Therefore only C and H atoms can be involved in these surface structures. By comparing our results to literature data we come to the conclusion that two scenarios are possible to explain the spectra observed for phases A and B.

(I) Phase A corresponds to the monohydride terminated surface, and phase B is a metastable, hydrogen-free unreconstructed [(2×1)-reconstructed but unrelaxed for (100)] surface.

(II) Phase A is due to multivalent hydrocarbon termination, and phase B corresponds to the monohydride surfaces.

For scenario I, the shift of the surface component in phase A (S_A) is induced by C-H bonds of the monoatomically terminated surfaces. A light-induced desorption of hydrogen from diamond (111) surfaces was observed by Pate *et al.*,⁴² and could therefore account for the decrease of the surface component in Fig. 4. However, given that phase A is characteristic of the hydrogen terminated surfaces, what surface structure is responsible for the C 1s spectra seen in phase B? On the (111) surface one can imagine a hydrogen-free, unreconstructed surface. Theoretical calculations come to different conclusions concerning the possibility that a metastable unreconstructed and hydrogen free (111) surface exists.^{9,30,43} Another possibility is that a small amount of hydrogen is left on the surface, not enough to be seen in the core-level spectra but sufficient to prevent a reconstruction of the (111) surface. Yamada and co-workers^{44,45} reported that a small amount of atomic hydrogen (equivalent to 5% of a monolayer) is sufficient to induce the (111) 2×1 → (111) 1×1:H transition. Studying the reverse process on the (111) surface Hamza, Kubiak, and Stulen⁴⁶ reported that *after* the desorption of hydrogen, further annealing is necessary to induce the reconstruction. This, however, is in contrast with the observations of Lee and Apai,⁴⁷ which were not able to remove the hydrogen completely from the (111) surface, even after the reconstruction took place.

The main argument against this interpretation for phases A and B, however, is the following: While for the (111) surface a reconstruction is necessary to go from phase A (H terminated 1×1) to phase C (H free, 2×1), no change of reconstruction is necessary in the same transition on the (100) surface, as witnessed by the LEED pattern. It is thus harder to imagine a metastable intermediate phase B on the (100) surface; and yet the corresponding C 1s core level signature (a single peak B) is observed on both surfaces.

For scenario II, emission from adsorbed hydrocarbons is responsible for the surface components S_A and S'_A in phase A. Again there are several possibilities left for phase B. The fact that the decrease of component S_A does not directly lead to the component S_C implies that (i) no dangling bonds are formed by the desorption of the adsorbates, or (ii) the mere existence of dangling bonds is not sufficient to induce the characteristic spectra of phase C. For the second alternative one is left with the same problems as before in scenario I. Case (i) might imply that either the adsorbates are only physisorbed on a monohydrogenated surface, or they are chemisorbed and an exchange reaction takes place, i.e., the desorp-

tion leads to a termination of the dangling bond by a hydrogen atom. Alternatively, the hydrocarbons might be cracked, part of the hydrogen desorbs, and the remaining C atoms form a hydrogen-terminated surface layer. Chin *et al.*⁴⁸ adsorbed methyl-radicals on the diamond (111) surface. The termination of the surface by methyl groups could be monitored by sum-frequency vibrational spectroscopy. Upon annealing at $T > 350$ °C, however, their spectra changed to the ones characteristic of the monohydrogenated surface. A similar process might occur in our experiment in going from phase A to phase B.

Methyl radicals are the most simple form of hydrocarbons which could be chemisorbed on the surfaces. Indeed, HREELS measurements on (111) surfaces which were grown homoepitaxially show vibrational modes characteristic of methyl groups.¹⁵ In scanning tunneling microscopy, protrusions are visible on homoepitaxial (111) surfaces which reveal a triangular structure, and they are interpreted as methyl groups.⁴⁹ Very recently Schober and Weis⁵⁰ observed, by STM, unreconstructed areas on a plasma-hydrogenated (111) surface on which each surface atom was saturated by a single methyl group, i.e., they provided evidence of an ordered C(111) 1×1:3H structure. The difference between the homoepitaxially grown surfaces and our samples prepared in a microwave hydrogen plasma lies only in the gas mixture used. In homoepitaxial growth a few percent of a carbon containing gas (in most cases methane) is added to the hydrogen plasma. Pressure and sample temperature are usually the same. In a recent paper, Rawles *et al.*⁵¹ stated that the effect of smoothing in a hydrogen plasma at sample temperatures below 975 °C is induced by surface diffusion and not by a simple etching of the surface. We do think that our surfaces may therefore be more similar to homoepitaxially prepared surfaces than to conventionally polished surfaces. The way adsorbates of methyl-radicals show up in C 1s core level spectra was investigated by Klauser *et al.*⁵² Indeed, a surface component shifted toward higher binding energies is visible in these spectra, however, the reported energy difference with respect to the bulk line amounts to 1.5 eV.

For the (100) orientation, for surfaces grown homoepitaxially^{15,53} or samples prepared in a microwave hydrogen plasma,¹⁴ no evidence for surfaces terminated other than by a single H per surface C atom has been reported so far. Nevertheless, we believe that the structure of the surfaces in the three phases can be described following scenario II as follows.

(i) The core-level spectra of phase A are characteristic of diamond surfaces that are partially covered by hydrocarbon molecules, possibly methyl groups, for which experimental evidence at least on (111) surfaces has already been given. Thus the surface core-level component S_A is due to emission from C atoms in adsorbed hydrocarbons.

(ii) Upon mild annealing ($T < 750$ °C), these adsorbates desorb or break up, and a monohydrogenated surface evolves (phase B). No distinct chemically shifted surface component has been resolved for this phase. As shown in Sec. III, a systematic study of the transition from phases B to C reveals a chemical shift of -0.15 eV between the surface and bulk atoms of phase B, which we consequently interpret as the chemical shift of the monohydride C-H groups. Note that

this chemical shift is opposite in sign from the one induced by the multivalent hydrogen termination of the adsorbates of phase A.

(iii) Annealing above the hydrogen desorption temperature leads to the clean diamond (100) and (111) surfaces (phase C), and the component S_C is therefore due to surface atoms that undergo the characteristic 2×1 Pandey chain reconstruction on the (111) or the relaxation to π -bonded dimers on the (100) surface.

(iv) Further annealing ($T > 1250$ °C) leads to a formation of a 4×1 reconstruction on the (100) surface; the (111) surface starts to graphitize (phase D) with the corresponding surface component S_D being very narrow (0.47 eV) and shifted by -1.13 eV with respect to the bulk component.

B. Kinetics of the transition of phases B \rightarrow C

The transition from phase B to phase C is the most interesting because it involves the reconstruction or relaxation of the hydrogen-free (111) or (100) surface, respectively. For scenario II the desorption of hydrogen is necessary in addition. Therefore, we have studied the kinetics of this transition in more detail on the polished (111) surface. As discussed in connection with Figs. 10 and 11, this transition is thermally activated and the relevant parameter is the activation energy E_{act} . If we assume that the appearance of the surface component S_C signals the transformation of a surface carbon atom from a state “ B_{surf} ” to a state “ S_C ,” the rate at which this transformation occurs is given by the Polanyi-Wigner equation

$$\frac{dn_S(t)}{dt} = -\frac{dn_B(t)}{dt} = n_B(t)^m \nu \exp[-E_{act}/(k_B T)]. \quad (1)$$

$n_S(t)$ [$n_B(t)$] is the number of surface atoms in state “ S_C ” (“ B_{surf} ”) per unit area, m the order of the phase transition with possible values from zero to two, ν the so-called attempt frequency (which is a true frequency only for $m=1$), T the surface temperature, and k_B the Boltzmann constant.

For a stepwise annealing as performed in our case the densities of atoms in state “ B_{surf} ” after two consecutive annealing steps $i-1$ and i are related according to

$$n_{B,i} = n_{B,i-1} \cdot \exp\{-\nu \Delta t_i \exp[-E_{act}/(k_B T_i)]\}, \quad (2)$$

where Δt_i is the duration and T_i the surface temperature of the annealing step i . This recursive equation can be derived by integrating Eq. (1), taking the activation energy E_{act} as constant, and assuming first-order kinetics ($m=1$). The double exponential factor

$$F_i = \exp\{-\nu \Delta t_i \exp[-E_{act}/(k_B T_i)]\} = n_{B,i}/n_{B,i-1} \quad (3)$$

just describes the decrease in the number of atoms still awaiting thermal conversion from state B_{surf} to S_C .

It is a safe assumption that the surface atoms n_B and n_S contribute with the same sensitivity to the photoemission sig-

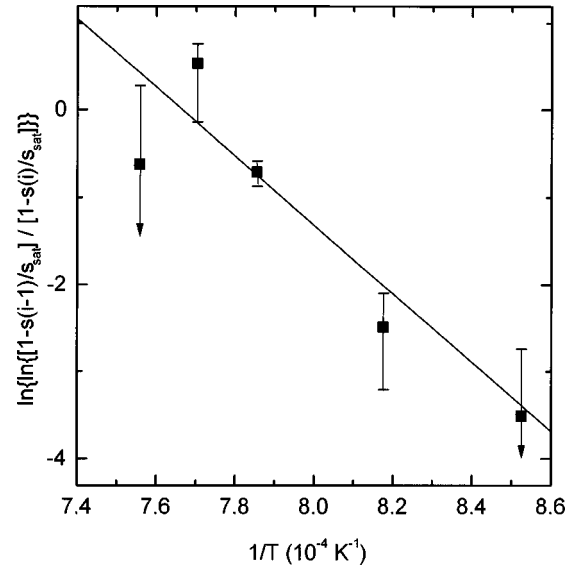


FIG. 14. Arrhenius plot for the conversion rate $F(T)$ of surface atoms from phase B to phase C [Eq. (7)]. For details, see text. The line corresponds to an activation energy of 3.4 eV, and an attempt to escape frequency of $7.5 \times 10^{10} \text{ s}^{-1}$.

nal during the whole phase transition, and that the contribution of bulk atoms to I_B remains constant. We then define the intensity ratio s :

$$s(t) := I_{S_C} / I_{tot} = \frac{n_S(t)}{N_{Surface} + N_{Bulk}} \quad (4)$$

where $N_{Surface}$ stands for the total number of surface atoms per unit area which remains constant during the phase transition: $N_{Surface} = n_B(t) + n_S(t) = \text{const}$. N_{Bulk} corresponds to the effective lateral density of atoms which contribute to the bulk signal.

By defining the saturation value s_{sat}

$$s_{sat} := \frac{I_{S_C}}{I_{tot}} \Big|_{T=1050 \text{ °C}} = \frac{N_{Surface}}{N_{Surface} + N_{Bulk}}, \quad (5)$$

one obtains a recursive equation similar to (2) for the intensity ratios s_i :

$$\frac{s_i}{s_{sat}} = 1 - F_i \left(1 - \frac{s_{i-1}}{s_{sat}} \right). \quad (6)$$

Using Eq. (3) the conversion of Eq. (6) into an Arrhenius representation yields

$$\ln \left[\ln \left(\frac{1 - s_{i-1}/s_{sat}}{1 - s_i/s_{sat}} \right) \right] = \ln(\nu \Delta t_i) - \frac{E_{act}}{k_B} \frac{1}{T_i}. \quad (7)$$

The parameters ν and E_{act} follow directly from a straight line fit when plotting the left-hand side of (7) versus $1/T_i$ (Fig.

14). For the attempt frequency and the activation energy, we obtain the best fit values of $\nu = 7.5 \times 10^{10 \pm 2} \text{ s}^{-1}$ and $E_{\text{act}} = 3.4 \text{ eV} \pm 0.4 \text{ eV}$, respectively. This activation energy is in good agreement with the activation energy of 3.5 eV for the desorption of hydrogen from the (111) surface of diamond obtained recently by Bobrov *et al.*⁵⁴ from temperature-programmed desorption measurements.

C. Sign and magnitude of the core-level shifts

Shifts in core-level binding energies are usually discussed in terms of initial- and final-state effects.⁵⁵ The initial-state contribution is that part of the chemical shift that would be obtained if binding energies were correctly described by Koopmans' theorem.⁵⁶ As such it takes into account the differences in the one electron Hartree-Fock potential seen by the different electron orbitals from which photoelectrons are emitted. In the simplest approximation the initial state shift can be estimated by the differences in the valence charge density of inequivalent atoms. The charge transfer in turn is related to differences in electronegativities of the bonding partners. Final state effects are related to the reaction of the remaining $(N-1)$ -electron system to the emission of the photoelectron (relaxation). If the relaxation energy of two systems can be assumed to be the same, core-level shifts reduce to initial-state shifts.⁵⁵

The core-level shift of component S_A cannot be explained in terms of a simple electrostatic initial-state shift. The electronegativity of hydrogen is lower than that of carbon (2.1 vs 2.5) on Pauling's scale.⁵⁷ A charge transfer from hydrogen to carbon, as expected by the respective electronegativities, is not unreasonable. It accounts for the negative electron affinity of hydrogen-terminated surfaces^{36,38,58-60} by forming a surface dipole layer which lowers the work function. The surface C atom is then expected to exhibit a surface core-level shift toward lower binding energies. This should hold for the monohydrogenated (111) and (100) surfaces (phase B) but even more for the adsorbed hydrocarbons (phase A). Indeed, we can deduce for the unresolved surface peak B_{surf} , which we attribute to C atoms bonded to H, a shift of 0.15 eV toward lower binding energy. However, for S_A , the component attributed to emission from the adsorbed hydrocarbons, a shift in the opposite direction is observed although the same electrostatic arguments as before are valid. This implies that the contribution of the relaxation energy to the chemical shift dominates.

The importance of the relaxation energy in photoelectron spectra of hydrocarbons was demonstrated by Pireaux *et al.*⁶¹ The C 1s binding energy of linear alkanes decreases with increasing chain length due to a more efficient screening of the photohole. Extending this result to a hydrocarbon molecule adsorbed on diamond, we would expect that the screening of the C 1s core hole located on the adsorbate is less efficient than for one on the surface of diamond where screening from the half-space of C atoms is possible. A small negative initial-state shift on account of the ionicity of the C-H bond is thus overcompensated for by the reduction in relaxation energy compared to the "bulk" diamond atoms. On the clean surfaces, however, a π bonding of the surface atoms evolves which leads to a more effective screening of a photohole at a surface atom compared to the bulk which

results in the rather large chemical shift of component S_C towards lower binding energies. Both arguments surmise, of course, that the initial state shift of surface C atoms that are only bonded to C, and have no dangling bond are negligible by comparison.

Finally, the difference in surface core-level shifts between the polished and the cleaved (111) surface after annealing at 1050° has to be explained. The maximum shift of the surface component S_C on the (111) surface is observed on the partially graphitized surface after annealing at $\approx 1250^\circ \text{C}$ (see Fig. 12 and Table II), and amounts to 1.13 eV. Virtually the same chemical shift is derived in Fig. 8 for the additional component from the fit of the spectrum taken on the cleaved surface. This component is missing on the polished surface (Fig. 8 and Table III). An obvious explanation would be that even at 1050° the cleaved surface is already partially graphitized. As it has been shown that a graphitization of the (111) surface starts at surface imperfections.^{62,63} The different behavior of the two surfaces might just reflect the differences in surface quality.

V. CONCLUSIONS

By studying the carbon 1s core level of single crystal diamond (100) and (111) surfaces polished in a hydrogen plasma, we were able to distinguish four different forms of surface termination. The as-prepared surfaces exhibit a surface core level which is shifted by 0.5–0.8 eV toward higher binding energy compared to emission from bulk carbon atoms. The intensity of this surface component depends sensitively on preparation conditions. We attribute this component to emission from adsorbed hydrocarbons. Upon annealing at 650 °C, the core-level spectra are characterized by a single line. We were not able to resolve a surface component; however, an indication for the true surface contribution is an apparent change in surface core-level shift between bulk line and surface component of the hydrogen-free (111) surface upon further annealing. From a consistent fit to a whole sequence of annealing steps, we deduce a surface core-level shift of -0.15 eV on the monohydrogenated (111) surface.

Annealing at 1050 °C leads to the spectra characteristic for the hydrogen-free, (2×1) -reconstructed (111) and (100) surfaces of diamond, which exhibit a surface component shifted towards lower binding energy by 0.8 and 0.9 eV for the (111) and (100) surfaces, respectively. Differences in the core-level spectra between a polished and a cleaved (111) sample can be explained by a partial graphitization of the cleaved surface. The transition from the monohydrogenated to the hydrogen-free, reconstructed surfaces is thermally activated with an activation energy of 3.4 eV, consistent with thermal-desorption experiments. Finally, at 1250 °C the (111) surface starts to graphitize. The emission from carbon atoms of graphitic areas appears at a binding energy -1.1 eV lower than the emission from the bulk diamond carbon atoms. Annealing temperatures of 1250 °C leads to a 4×1 reconstruction on the (100) surface; a model for this reconstruction is lacking.

The signs and magnitudes of the core-level shifts, notably of the component which is attributed to adsorbed hydrocarbons cannot be explained in terms of a simple initial-state shift. Therefore we conclude that on diamond surfaces the relaxation energy, i.e., the response of the surrounding elec-

tron system to the formation of the photohole is the dominant term responsible for the surface core-level binding-energy shifts.

ACKNOWLEDGMENTS

We would like to thank K. Janischowsky and R. Stöckel for the hydrogen plasma preparation of our samples. The

authors gratefully acknowledge financial support by the Deutsche Forschungsgemeinschaft (Project No. Le 643/5-2) carried out under the auspices of the trinational "D-A-CH" cooperation of Germany, Austria, and Switzerland on the "Synthesis of Superhard Materials." The measurements at BESSY were supported by the Bundesminister für Bildung, Wissenschaft, Forschung und Technologie under Contract No. 05 622 WEA 7.

- ¹G. Le Lay, V. Y. Aristov, and M. Fontaine, *Prog. Surf. Sci.* **48**, 145 (1995).
- ²E. Landemark, C. J. Karlsson, Y. C. Chao, and R. I. G. Uhrberg, *Phys. Rev. Lett.* **69**, 1588 (1992).
- ³J. J. Paggel, W. Theis, K. Horn, Ch. Jung, C. Hellwig, and H. Petersen, *Phys. Rev. B* **50**, 18 686 (1994).
- ⁴C. J. Karlsson, E. Landemark, Y. C. Chao, and R. I. G. Uhrberg, *Phys. Rev. B* **50**, 5767 (1994).
- ⁵K. Hricovini, R. Günther, P. Thiry, A. Taleb-Ibrahimi, G. Idlekofer, J. E. Bonnet, P. Dumas, Y. Petroff, X. Blase, X. Zhu, S. G. Louie, Y. J. Chabal, and P. A. Thiry, *Phys. Rev. Lett.* **70**, 1992 (1993).
- ⁶C. J. Karlsson, F. Owman, E. Landemark, Y. C. Chao, P. Mårtensson, and R. I. G. Uhrberg, *Phys. Rev. Lett.* **72**, 4145 (1994).
- ⁷P. Krüger and J. Pollmann, *Phys. Rev. Lett.* **74**, 1155 (1995).
- ⁸C. Kress, M. Fiedler, W. G. Schmidt, and F. Bechstedt, *Phys. Rev. B* **50**, 17 697 (1994).
- ⁹B. N. Davidson and W. E. Pickett, *Phys. Rev. B* **49**, 11 253 (1994).
- ¹⁰Y. L. Yang and M. P. D'Evelyn, *J. Vac. Sci. Technol. A* **10**, 978 (1992).
- ¹¹Z. Zhang, M. Wensell, and J. Bernholc, *Phys. Rev. B* **51**, 5291 (1995).
- ¹²G. Kern, J. Hafner, J. Furthmüller, and G. Kresse, *Surf. Sci.* **352-354**, 745 (1996).
- ¹³J. Furthmüller, J. Hafner, and G. Kresse, *Phys. Rev. B* **53**, 7334 (1996).
- ¹⁴B. D. Thoms and J. E. Butler, *Surf. Sci.* **328**, 291 (1995).
- ¹⁵T. Aizawa, T. Ando, M. Kamo, and Y. Sato, *Phys. Rev. B* **48**, 18 348 (1993).
- ¹⁶T. Tsuno, T. Imai, Y. Nishibayashi, K. Hamada, and N. Fujimori, *Jpn. J. Appl. Phys.* **30**, 1063 (1991).
- ¹⁷C. Nützenadel, O. M. Küttel, L. Diederich, E. Maillard-Schaller, O. Gröning, and L. Schlapbach, *Surf. Sci.* **369**, L111 (1996).
- ¹⁸B. D. Thoms, M. S. Owens, J. E. Butler, and C. Spiro, *Appl. Phys. Lett.* **65**, 2957 (1994).
- ¹⁹O. M. Küttel, L. Diederich, E. Schaller, O. Carnal, and L. Schlapbach, *Surf. Sci.* **337**, L812 (1995).
- ²⁰M. D. Winn, M. Rassinger, and J. Hafner, *Phys. Rev. B* **55**, 5364 (1997).
- ²¹T. Frauenheim, U. Stephan, P. Blaudeck, D. Porezag, H. G. Busmann, W. Zimmermann-Edling, and S. Lauer, *Phys. Rev. B* **48**, 18 189 (1993).
- ²²Z. Jing and J. L. Whitten, *Surf. Sci.* **314**, 300 (1994).
- ²³J. B. Marsh and H. E. Farnsworth, *Surf. Sci.* **1**, 3 (1964).
- ²⁴P. G. Lurie and J. M. Wilson, *Surf. Sci.* **65**, 453 (1977).
- ²⁵A. V. Hamza, G. D. Kubiak, and R. H. Stulen, *Surf. Sci.* **237**, 35 (1990).
- ²⁶S. H. Yang, D. A. Drabold, and J. B. Adams, *Phys. Rev. B* **48**, 5261 (1993).
- ²⁷K. C. Pandey, *Phys. Rev. B* **25**, 4338 (1982).
- ²⁸H. Kawarada, *Surf. Sci. Rep.* **26**, 205 (1996).
- ²⁹G. Kern, J. Hafner, and G. Kresse, *Surf. Sci.* **366**, 464 (1996).
- ³⁰A. Scholze, W. G. Schmidt, and F. Bechstedt, *Phys. Rev. B* **53**, 13 725 (1996).
- ³¹B. B. Pate, M. Oshima, J. A. Silberman, G. Rossi, I. Lindau, and W. E. Spicer, *J. Vac. Sci. Technol. A* **2**, 957 (1984).
- ³²J. F. Morar, F. J. Himpsel, G. Hollinger, J. L. Jordan, G. Hughes, and F. R. McFeely, *Phys. Rev. B* **33**, 1340 (1986).
- ³³R. Graupner, J. Ristein, and L. Ley, *Surf. Sci.* **320**, 201 (1994).
- ³⁴R. Klauser, J. M. Chen, T. J. Chuang, L. M. Chen, M. C. Shih, and J. C. Lin, *Surf. Sci.* **356**, L410 (1996).
- ³⁵J. Wu, R. Cao, X. Yang, P. Pianetta, and I. Lindau, *J. Vac. Sci. Technol. A* **11**, 1048 (1993).
- ³⁶G. Franz and P. Oelhafen, *Surf. Sci.* **329**, 193 (1995).
- ³⁷V. S. Smentkowski, H. Jnsch, M. A. Henderson, and J. T. Yates, *Surf. Sci.* **330**, 207 (1995).
- ³⁸L. Diederich, O. M. Küttel, E. Schaller, and L. Schlapbach, *Surf. Sci.* **349**, 176 (1996).
- ³⁹R. Graupner, M. Hollering, A. Ziegler, J. Ristein, L. Ley, and A. Stampfl, *Phys. Rev. B* **55**, 10 841 (1997).
- ⁴⁰D. A. Shirley, *Phys. Rev. B* **5**, 4709 (1972).
- ⁴¹O. Keski-Rahkonen and M. O. Krause, *At. Data Nucl. Data Tables* **14**, 139 (1974).
- ⁴²B. B. Pate, M. H. Hecht, C. Binns, I. Lindau, and W. E. Spicer, *J. Vac. Sci. Technol.* **21**, 364 (1982).
- ⁴³G. Kern, J. Hafner, and G. Kresse, *Surf. Sci.* **366**, 445 (1996).
- ⁴⁴Y. Mitsuda, T. Yamada, T. J. Chuang, H. Seki, R. P. Chin, J. Y. Huang, and Y. R. Shen, *Surf. Sci.* **257**, L633 (1991).
- ⁴⁵H. Seki, T. Yamada, T. J. Chuang, R. P. Chin, J. Y. Huang, and Y. R. Shen, *Diamond Relat. Mater.* **2**, 567 (1993).
- ⁴⁶A. V. Hamza, G. D. Kubiak, and R. H. Stulen, *Surf. Sci.* **206**, L833 (1988).
- ⁴⁷S. T. Lee and G. Apai, *Phys. Rev. B* **48**, 2684 (1993).
- ⁴⁸R. P. Chin, J. Y. Huang, Y. R. Shen, T. J. Chuang, and H. Seki, *Phys. Rev. B* **54**, 8243 (1996).
- ⁴⁹H. Sasaki and H. Kawarada, *Jpn. J. Appl. Phys.* **32**, L1771 (1993).
- ⁵⁰G. Schober and O. Weis, *Surf. Sci.* **383**, 203 (1997).
- ⁵¹R. E. Rawles, S. F. Komarov, R. Gat, W. G. Morris, J. B. Hudson, and M. P. D'Evelyn, *Diamond Relat. Mater.* **6**, 791 (1997).
- ⁵²R. Klauser, T. J. Chuang, L. A. Smoliar, and W.-T. Tzeng, *Chem. Phys. Lett.* **255**, 32 (1996).
- ⁵³T. Aizawa, T. Ando, K. Yamamoto, M. Kamo, and Y. Sato, *Diamond Relat. Mater.* **4**, 600 (1995).
- ⁵⁴K. Bobrov, B. Fisgeer, H. Shechter, M. Folman, and A. Hoffman, *Diamond Relat. Mater.* **6**, 736 (1997).

- ⁵⁵N. Mårtensson and A. Nilsson, *J. Electron Spectrosc. Relat. Phenom.* **75**, 209 (1995).
- ⁵⁶T. Koopmans, *Physica (Amsterdam)* **1**, 104 (1933).
- ⁵⁷L. N. Pauling, *The Nature of the Chemical Bond and the Structure of Molecules and Crystals*, 3rd ed. (Cornell University Press, Ithaca, NY, 1986).
- ⁵⁸F. J. Himpsel, J. A. Knapp, J. A. VanVechten, and D. E. Eastman, *Phys. Rev. B* **20**, 624 (1979).
- ⁵⁹B. B. Pate, W. E. Spicer, T. Ohta, and I. Lindau, *J. Vac. Sci. Technol.* **17**, 1087 (1980).
- ⁶⁰J. Ristein, W. Stein, and L. Ley, *Phys. Rev. Lett.* **78**, 1803 (1997).
- ⁶¹J. J. Pireaux, S. Svensson, E. Basilier, P.-A. Malmqvist, U. Gelius, R. Caudano, and K. Siegbahn, *Phys. Rev. A* **14**, 2133 (1976).
- ⁶²B. N. Davidson and W. E. Pickett, *Phys. Rev. B* **49**, 14 770 (1994).
- ⁶³G. Jungnickel, C. D. Latham, M. I. Heggie, and T. Frauenheim, *Diamond Relat. Mater.* **5**, 102 (1996).